Molecular Crystals and Liquid Crystals
Publication details, including instructions for authors and subscription information:
http://www.tandfonline.com/loi/gmcl20

Optical, Electro-Optical, and Dielectric Properties of Acrylic Tripropyleneglycol Based Polymer Network Systems Including LCs

Y. Derouiche [a b d], K. Koynov [b], F. Dubois [c], R. Douali [c], C. Legrand [c] & U. Maschke [a]

[a] Unité Matériaux et Transformations (UMET), UMR 8207-CNRS, Bâtiment C6, Université Lille 1 - Sciences et Technologies, 59655 Villeneuve d'Ascq Cedex, France

[b] Max-Planck Institute of Polymer Research, Postfach 3148, 55021 Mainz, Germany

[c] UDSMM, Université du Littoral - Côte d'Opale, 62228 Calais, France

[d] Laboratoire des dispositifs des micro-ondes et matériaux pour les énergies renouvelables, Université ZIANE Achour, 17000 Djelfa, Algeria

Version of record first published: 13 Jun 2012.

To cite this article: Y. Derouiche , K. Koynov , F. Dubois , R. Douali , C. Legrand & U. Maschke (2012): Optical, Electro-Optical, and Dielectric Properties of Acrylic Tripropyleneglycol Based Polymer Network Systems Including LCs, Molecular Crystals and Liquid Crystals, 561:1, 124-135

To link to this article: http://dx.doi.org/10.1080/15421406.2012.687149

Mol. Cryst. Liq. Cryst., Vol. 561: pp. 124–135, 2012

ISSN: 1542-1406 print/1563-5287 online
DOI: 10.1080/15421406.2012.687149

Taylor & Francis
Taylor & Francis Group

Optical, Electro-Optical, and Dielectric Properties of Acrylic Tripropyleneglycol Based Polymer Network Systems Including LCs

Y. DEROUICHE,[1,2,4] K. KOYNOV,[2] F. DUBOIS,[3] R. DOUALI,[3] C. LEGRAND,[3] AND U. MASCHKE[1,*]

[1]Unité Matériaux et Transformations (UMET), UMR 8207–CNRS, Bâtiment C6, Université Lille 1 – Sciences et Technologies, 59655 Villeneuve d'Ascq Cedex, France
[2]Max-Planck Institute of Polymer Research, Postfach 3148, 55021 Mainz, Germany
[3]UDSMM, Université du Littoral – Côte d'Opale, 62228 Calais, France
[4]Laboratoire des dispositifs des micro-ondes et matériaux pour les énergies renouvelables, Université ZIANE Achour, 17000 Djelfa, Algeria

Polymer/liquid crystal (LC) films were elaborated by photopolymerization using UV radiation of mixtures made up of a LC, a monomer and a photoinitiator. Three acrylic difunctional tripropyleneglycol based monomers possessing the same chemical structures were studied. The monomer/LC films exhibit distinguished morphologies presenting specific LC domain sizes, which were observed by polarized optical microscopy. These results were correlated with the electro-optical responses of the corresponding polymerized/crosslinked systems. A detailed characterization by linear dielectric spectroscopy of monomers and corresponding polymers was carried out as a function of temperature in the frequency range from 20 Hz to 1 MHz.

Keywords Dielectric spectroscopy; electro-optical characterization; liquid crystal; phase separation; polymer

1. Introduction

Mixtures of a polymer with liquid crystal (LC) molecules of low molecular weight can lead to homogeneous or heterogeneous systems. In the latter case, phase separation (demixing) occurs and the resulting material may consist of a crosslinked polymer network in a continuous LC phase called NPLC (Polymer Network LC). When the polymer/LC composite is formed of a dispersion of LC droplets in a continuous macromolecular phase, it is called PDLC (Polymer Dispersed Liquid Crystal) [1]. PDLCs represent a relatively new class of materials with interesting properties [5–9] which consist generally of a dispersion of micro- or nanodomains of a nematic LC in a polymer matrix. Several methods

*Address correspondance to U. Maschke, Unité Matériaux et Transformations (UMET), CNRS UMR 8207, Université Lille1 – Sciences et Technologies, 59655 Villeneuve d'Ascq Cedex, France. Tel: 0033 3 20 33 63 81; Fax: 0033 3 20 43 43 45. E-mail: ulrich.maschke@univ-lille1.fr

are used for the preparation of PDLC films, including the processes leading to phase separation techniques [1,10]. A homogeneous blend composed of a LC of low molecular weight and a monomer will be polymerized/crosslinked, leading to the formation of segregation LC by Polymerization Induced Phase Separation (PIPS). Other methods include either sample treatment by temperature variation (TIPS: Thermally Induced Phase Separation), or by evaporation of a solvent (SIPS: Solvent Induced Phase Separation). However SIPS and TIPS methods are restricted to a limited number of polymer/LC systems. In the case of the PIPS method, the polymerization of the monomers can be achieved thermally or photochemically by ultraviolet radiation, or by electron bombardment. When the LC domain size in the polymer matrix is in the order of micrometers, the corresponding polymer/LC systems are called micro-PDLC. These micro-PDLCs are electroactive particularly in the wavelength range of visible light, and switch under the action of an electric field from an incident scattering state to a transparent state. These systems are promising materials for electro-optic applications such as flexible displays and light shutter devices [1–5].

The aim of this work is to discuss various optical, electro-optical, thermal and dielectric properties of samples made from propyleneglycol based acrylic systems and also to study the correlation between the morphology of the starting mixtures before polymerization and the electro-optical properties of the final products (PDLCs). The propyleneglycol diacrylate monomers employed in this study are distinguished by their molecular weight between the two reactive chain ends, giving the formation of polymer networks with varying distances between two adjacent crosslinking points

2. Materials and Experimental Methods

2.1. Materials

Three acrylic difunctional propyleneglycol based monomers possessing the same chemical structures were used in this study; differing only by their chain lengths in terms of their molecular weight: Tripropyleneglycoldiacrylate (TPGDA) with $M_n = 300$ g/mol, polypropyleneglycoldiacrylate with $M_n = 540$ g/mol (PPGDA540), and polypropyleneglycoldiacrylate with $M_n = 900$ g/mol (PPGDA900); M_n being the number average of the molecular weight.

Samples were prepared from mixtures of X weight-percent (wt.-%) LC and (100-X) wt.-% of the monomer. 2wt.-% (compared to the acrylate) of 2-hydroxy-2-methyl-1-phenyl-propane-1-one (Darocur 1173) was added as photoinitiator to the initial mixtures before exposure to UV light. All products were used as received.

The nematic LC used in this work is the eutectic mixture E7 (Merck Japan) containing four cyanoparaphenylene derivatives. E7 is made of 51 weight-percent (wt.-%) 4-cyano-4′-pentylbiphenyl (5CB), 25 wt.-% 4-cyano-4′-heptyl-biphenyl (7CB), 16 wt.-% 4-cyano-4′-octyloxybiphenyl (8OCB), and 8 wt.-% 4-cyano- 4′′-pentyl-p-terphenyl (5CT). This LC mixture exhibits a nematic-isotropic transition temperature at $T_{NI} = 61^{\circ}$C and a positive dielectric anisotropy $\Delta\varepsilon = \varepsilon_{\parallel} - \varepsilon_{\perp}$ at T = 20°C, where $\varepsilon_{\parallel}$ and $\varepsilon_{\perp}$ represent the parallel and perpendicular dielectric constants, respectively. The refractive indices of E7 at T = 20°C are given as $n_0 = 1.5183$; $n_e = 1.7378$ ($\lambda = 632.8$ nm) [11,12], leading to a birefringence of $\Delta n = n_e - n_0 = 0.2195$. The chemical structures of the compounds are given in Fig. 1.

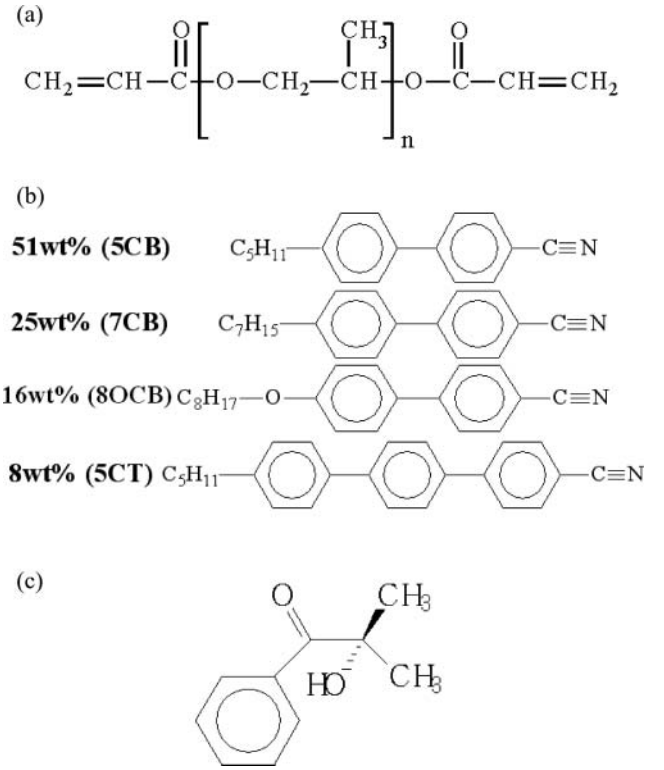

Figure 1. Chemical structures of (a) Polypropyleneglycoldiacrylate PPGDA, (b) the nematic LC mixture E7, (c) the photoinitiator 2-hydroxy-2-methyl-1-phenyl-propane-1-one (Darocur 1173).

2.2. Experimental Methods

2.2.1. Dielectric Spectroscopy. The dielectric characterization set-up was made of a HP4284A (20 Hz–1 MHz) impedance analyser, and a measuring cell which allowed to achieve measurements in the frequency range from 20 Hz to 1 MHz. The measuring ac-voltage is fixed to 0.1 V_{rms}. The real $\varepsilon'(f)$ and imaginary $\varepsilon''(f)$ parts of the complex permittivity ε^* ($\varepsilon^*(f) = \varepsilon'(f) - j\varepsilon''(f)$) were calculated from the measured capacitance C and conductance G:

$$\varepsilon'(f) = \frac{C(f)}{C_0}, \quad \varepsilon''(f) = \frac{G(f)}{2\pi f C_0} \tag{1}$$

where C_0 is the empty cell capacitance measured before cell filling. The temperature was stabilized with a temperature controller (Oxford Instrument ITC601 with platinum sensor) with an accuracy better than 0.1°C, and the experimental set-up was controlled via a micro-computer equipped with HPVEE software.

The measuring cell for dielectric spectroscopy consists of a planar capacitor made of two glass plates [13]. To obtain an electrical contact, the first plate was covered by gold and the second one by ITO (Indium Tin Oxide). The ITO is transparent and allows checking the filling of the cell which was carried out by capillarity. The sample thickness was fixed with mica or double-sided self-adhesive tape spacers (25 μm). The electrical contact on the electrodes was made with coaxial connectors (SMA standard). For the pure LC, the

dielectric characterization is usually carried out using orientation layers whereas the PDLC material does not require any orientation layers.

To cure the initial reactive mixtures, two fluorescent lamps of type TL08 (Philips) were employed as UV light source. This monochromatic light source with a wavelength of $\lambda = 365$ nm, and a power output of 1.5 mW/cm^2, requires exposure times of some minutes up to half an hour. Due to its weak power output, this UV equipment leads to a relatively slow photopolymerization process. Exposure to UV irradiation was conducted at room temperature without humidity rate control.

2.2.2. Polarized Optical Microscopy (POM) Measurements. An Olympus BX-41 microscope equipped with a heating-cooling stage from Linkam was employed as polarized optical microscopy (POM). First, the samples prepared as mentioned earlier were submitted to a heating rate of 2°C/min from room temperature to 30°C above the transition temperature leading to the isotropic phase. Samples were then left approximately 5 min in the isotropic state. The samples were then cooled down at a rate of –2°C/min.

2.2.3. Electro-Optical Measurements. The electro-optical experiments were performed at room temperature by measuring the transmission of unpolarized HeNe laser light at a wavelength of $\lambda = 632.8$ nm. The polymer/LC films were elaborated between ITO coated glass plates which were oriented normal to the laser beam. The distance between the sample cell and the detector (silicon photodiode) was approximately 30cm. The collection angle of the transmitted intensity was about 2°, so that principally forward scattering was detected.

The intensity of transmitted light was recorded on a micro-computer using an interface card (DAS 1600-2). The output of a frequency generator was amplified and used to drive the shutter device. Starting from the electrical off-state, the applied sinusoidal voltage of frequency 1 kHz was increased continuously up to a desired maximum value Vmax. Subsequently it was decreased in the same way. The whole scan up and down ramp was usually performed during 120 s, an additional measuring time of 60 s allows to follow the relaxation behavior of the transmittance in the off-state.

Average values of PDLC film thicknesses were calculated by taking into account the difference of the total thickness of the electro-optical cell (with glass slides) and the sum of the thicknesses of each glass slide individually. The thickness measurements were taken at several locations on the cell by a caliper rule of high precision.

2.2.4. Differential Scanning Calorimetry (DSC). The Differential Scanning Calorimetry (DSC) technique was used for the study of polymer/LC materials [14–18] and in particular to detect phase transitions for low molecular weight molecules such as the nematic LC E7. DSC measurements were performed on a Perkin Elmer Pyris Diamond calorimeter equipped with an Intracooler 2P system allowing cooling experiments. Samples for calorimetric measurements were prepared by introducing approximately 8 mg of the material into an aluminum DSC pan, which was sealed to avoid evaporation effects during the temperature treatment. A rate of 10°C/min (heating and cooling) was used in the temperature range from 70 to 100°C. The program consists first in cooling the sample followed by three heating and cooling cycles to take into account eventual thermal events related to the sample preparation history. The results presented in this work were obtained from the first heating ramps. In each case, at least three duplicate samples having the same composition and prepared independently were used to check the reproducibility of results. The polymer glass transition temperature was determined from the midpoint of the transition range of the thermograms.

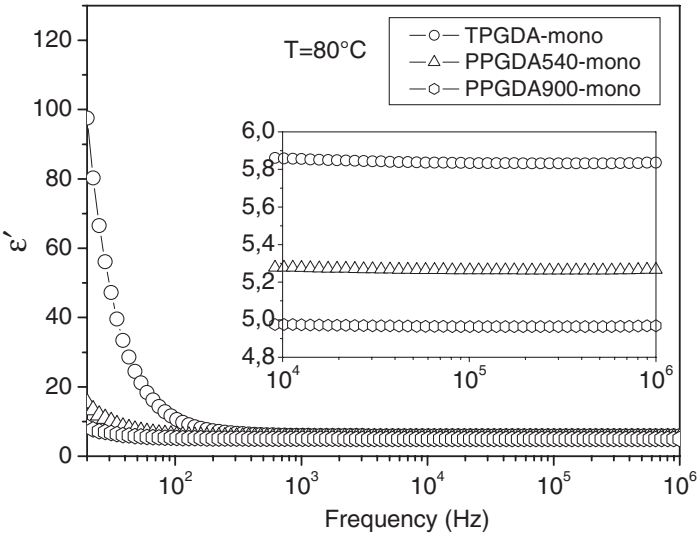

Figure 2. Real part of the dielectric spectra of the three monomers, TPGDA, PPGDA540 and PPGDA900.

3. Results and Discussion

3.1. Dielectric Spectroscopy

The dielectric measurements were performed on several samples of the same material exhibiting different thicknesses. The results shown here represent average values calculated from different samples. For each given monomer, the difference of the permittivity of the samples did not exceed 6%. Figure 2 represents dielectric spectra of the three monomers obtained at a temperature of 80°C. For the TPGDA monomer, the plot ε'(f) contains two frequency ranges with different behavior: At high frequencies (f > 1 kHz), ε' does not depend on the frequency and the measured value ($\varepsilon'(80^\circ C) = 5.83$) corresponds to the static value of the dielectric constant of the monomer. At low frequencies, due to the accumulation of ionic charges near electrodes, ε' increases with frequency. This effect is lower for PPGDA540 and PPGDA900 monomers which present probably low concentrations of ionic impurities. When the molecular weight of the monomer increases, TPGDA < PPGDA540 < PPGDA900, the static dielectric constant went down (at T = 80°C: $\varepsilon' = 5.26$ for PPGDA540, $\varepsilon' = 4.96$ for PPGDA900); this behaviour can be explained by the decrease of the C=O carbonyl group density. Indeed, the dipolar moment of the monomers is dominated by that of the C=O group. Figure 1 shows that the three molecules present similar chemical structures with two carbonyl groups and only the chain length changes. It can concluded that the density of carbonyl group decreases when the molecular weight increases. An estimation of the C=O group density can be obtained using formula (2). The results of the calculations are summarized in Table 1 using the values of the density given by the supplier (d = 1.03 g/ml for TPGDA, d = 1.02 g/ml for PPGDA540, d = 1.01 g/ml for PPGDA900):

$$N_{C=O} = 2N_A \frac{d}{M_W} \tag{2}$$

Table 1. Characterization of the samples under investigation. The molecular weight was calculated by the ^{1}H NMR method, and the glass transition temperature T_g was determined by DSC measurements. N_A is the Avogadro number

Monomer type	M_W (g/mol)	Density d (g/ml)	$N_{C=0}$ (mol^{-1})	Conductivities ($\times 10^{-8}(\Omega.m)^{-1}$	T_g (°C)
TPGDA	348	1.03	3.568×10^{21}	160	−85
PPGDA540	516	1.02	2.381×10^{21}	27	−74
PPGDA900	870	1.01	1.398×10^{21}	9.3	−70

The three monomers do not present any relaxation processes in the explored frequency and temperature range. Particularly, the α-relaxation was not observed due to the low glass transition temperature of these monomers, compared to the room temperature. The conductivity effect, related to the accumulation of ionic charges near electrodes, was found to be more pronounced for TPGDA and PPGDA540 compared to PPGDA900 (see Table 1). This is in good agreement with the evolution of the ionic conductivity, which is more important for these two monomers compared to PPGDA900 [20].

Figure 3 shows the Arrhenius plot of the conductivity of the polymerized/crosslinked PPGDA900/E7 system as function of the LC concentration. The conductivity σ increases with temperature due to thermal agitation effects which facilitates the migration of charges. It could also been observed that the conductivity increases with the E7 – concentration, which can be explained by the enhanced number of charges in segregated domains of E7.

This investigation was performed in the temperature range from 25°C to 100°C allowing to determine the evolution of different parameters. Figure 3 represents the classical plots $\ln(\sigma)$ versus 1/T, where a linear dependence of $\ln(\sigma)$ versus 1/T was observed in region (1), indicating that the conductivity exhibits an activated behaviour, which can be

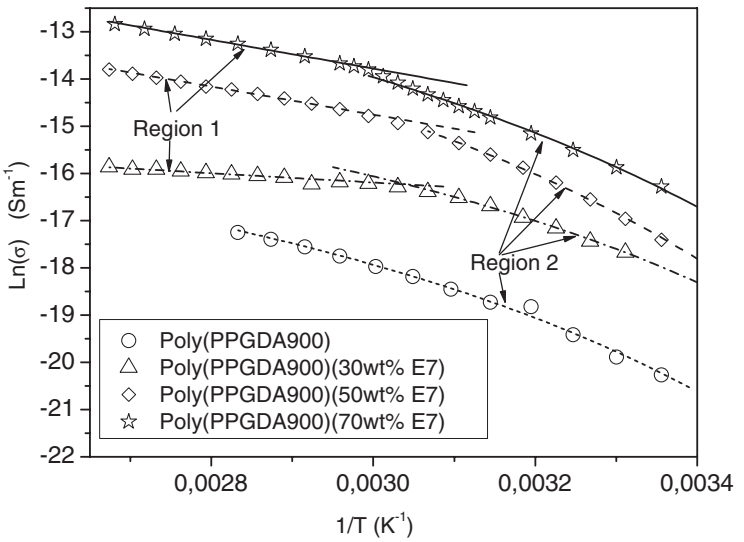

Figure 3. Temperature dependence of the conductivity of the Poly(PPGDA900)/E7 system as a function of LC concentration.

Table 2. Results from fitting procedures concerning Arrhenius and VTF parameters of the poly(PPGDA 900)/E7 system

	Arrhenius		VTF		
	σ_0 (Sm^{-1})	E_a (eV)	σ_1 ($SK^{1/2}m^{-1}$)	E_V (eV)	T_0 (K)
Poly(PPGDA900)			4.35×10^{-5}	0.047	223
Poly(PPGDA900)(30wt%E7)	1.79×10^{-6}	0.085	1.27×10^{-4}	0.039	223
Poly(PPGDA900)(50wt%E7)	1.29×10^{-3}	0.223	1.35×10^{-3}	0.049	215
Poly(PPGDA900)(70wt%E7)	9.81×10^{-3}	0.263	4.51×10^{-3}	0.057	215

described by the Arrhenius relation [21–24]:

$$\sigma = \sigma_0 \exp\left[\frac{-E_a}{kT}\right] \tag{3}$$

where σ_0 is the pre-exponential factor, E_a stands for the activation energy for thermally activated processes and k represents the Boltzmann constant. The region 2 in figure 3 corresponds to low temperatures; the curves are not linear and the conductivity shows a typical Vogel-Tamman-Fulcher (VTF) relationship [21,25–28]:

$$\sigma = \sigma_1 T^{-\frac{1}{2}} \exp\left[\frac{-E_V}{k(T - T_0)}\right] \tag{4}$$

where σ_1, E_v and T_0 are fitting parameters which are related to the carrier density, pseudo activation energy and zero configuration entropy of the chains, respectively [21]. T_0 represents an ideal glass transition temperature at which the conductivity goes to zero [29–30], and was chosen as half of the sum of the glass transition temperatures of monomer and segregated domains of E7, respectively. The results of the fitting procedures for the poly (PPGDA500)/E7 system and the pure polymer, obtained from Arrhenius and VTF processes, are summarized in Table 2.

The evolution of the conductivity versus temperature indicates a change in the transport mechanism. The VTF behavior observed at low temperatures, reported in previous works, was devoted to the study of the ionic conduction in polymer electrolytes [25,29,31]. The authors suggested that the ion conduction follows the Williams-Landel-Ferry (WLF) mechanism [31,32], which means that the ion transport is correlated with the segmental motion of the polymer chains [31,33]. Thus it can be suggested that the difference observed from the VTF behaviour of the PPGDA/E7 system is linked to the variation of the LC concentration. It was observed as well, that the PPGDA/E7 system shows a rapid decrease of the conductivity in the vicinity of the nematic-isotropic transition temperature of the LC domains.

3.2. Polarized Optical Microscopy

The observations by polarized optical microscopy were performed by varying temperature and concentration of the nematic LC E7, covering the range from 50 wt.-% to 100 wt.-% of E7. In order to visualize the segregated LC domains in the (nematic +isotropic) phase, Fig. 4 shows the morphology corresponding to the monomeric PPGDA540/E7 system at

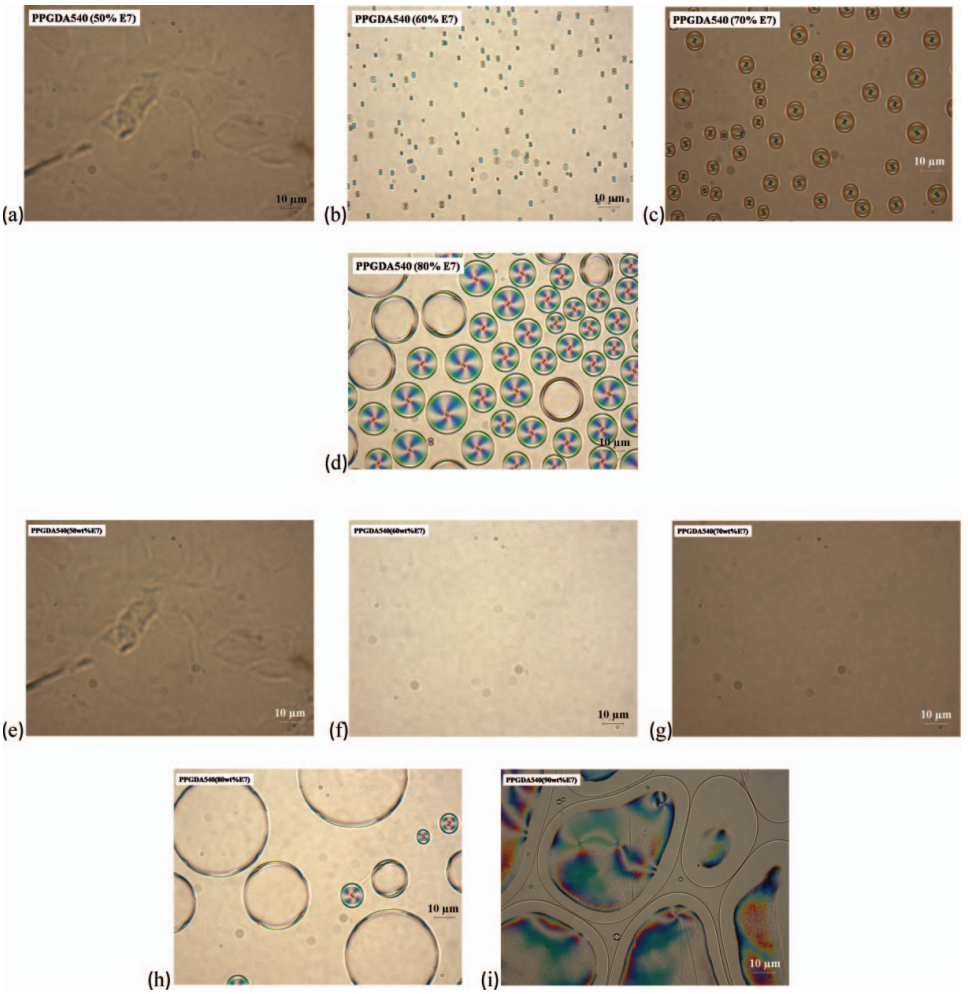

Figure 4. Variation of the morphology of the (PPGDA540/E7) system at T = 0°C (Figs. 4a–d) and T = 25°C (Figs. 4e–i), according to the change in composition.

temperatures of 0°C and 25°C, for different E7 concentrations. The micrographs reveal a clear variation of the LC domain sizes in the nematic state, depending on the concentration of E7. Photos taken at T = 0°C (Figs. 4a–d) show phase separation effects above 50 wt.-% of E7. At T = 25°C, corresponding to Figs. 4e–i, the phase separation is observed for systems where the LC concentration is higher than 60 wt.-% —for lower concentrations the system remains in the isotropic phase. The micrographs taken at 70, 80, and 90 wt.-% show that the two phases (N+I) coexist. The brighter regions indicate the isotropic phase, while the domains with a geometric shape with dark colors represent the nematic droplets dispersed in the monomer PPGDA 540 (parallel polarizer/analyzer). It is evident that the size of LC domains increases with the E7 concentration. The choice of the right monomeric mixture is crucial in terms of the phase separation induced by PIPS: good electro-optical results can generally be obtained if the initial reactive blend is in the homogeneous isotropic phase, close to the limit of phase separation.

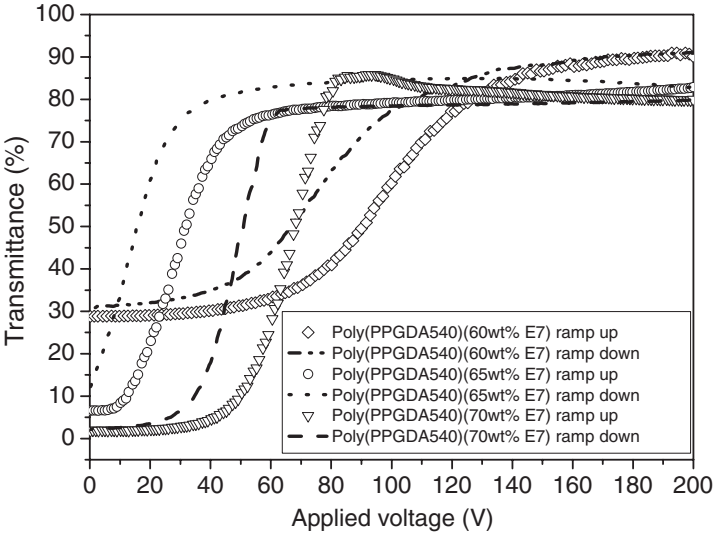

Figure 5. Optical transmittance of poly(PPGDA540)/E7 films exhibiting thicknesses between 17 and 20 microns.

3.3. Electro-Optical Studies

Selected representative poly (PPGDA540)/E7 films, possessing thicknesses varying between 17 and 20 μm, were analyzed by carrying out electro-optical measurements. The optical transmittance of these poly (PPGDA540)/E7 films is shown in Fig. 5 as a function of the applied voltage. Increasing the LC concentration from 60 to 70 wt.-% provokes a reduction of the transmittance in the OFF-state. This result is not surprising since when the amount of LC becomes more important in the film, the number of LC domains increases which act as scattering objects. The light is more diffused in the film which reduces the transmittance in the absence of the electrical field. The transmittance in the ON-state remains the same for films of both 65 and 70 wt.-% LC. The threshold and saturation voltages decrease from 60 to 65 wt.-% E7 and they grow up for the 70 wt.-% LC system. These samples represent a relatively large hysteresis effect which increases with concentration of LC [19]. The poly(PPGDA540)/E7 film with 65 wt.-% of E7 has a relatively low memory effect i.e. the transmittance does not return to the initial state when the electric field is off [19].

3.4. Differential Scanning Calorimetry

Figures 6 and 7 represent respectively the variation of the glass transition temperatures of LC and polymer matrix as a function of E7 concentration, for the three systems considered. The glass transition of the LC remains almost constant around $T = -65^{\circ}C \pm 1^{\circ}C$ regardless of the chosen system, and independent of the composition. This suggests that the LC phase inside the segregated domains is essentially pure and contains no dissolved residual monomer. This result also confirms that the molecular weight of the monomers does not affect the glass transition of E7. On the other hand the glass transition temperature of the polymer matrix obtained from the three systems differs from one system to another. The poly(TPGDA) presents the highest density of crosslinking points of the three networks,

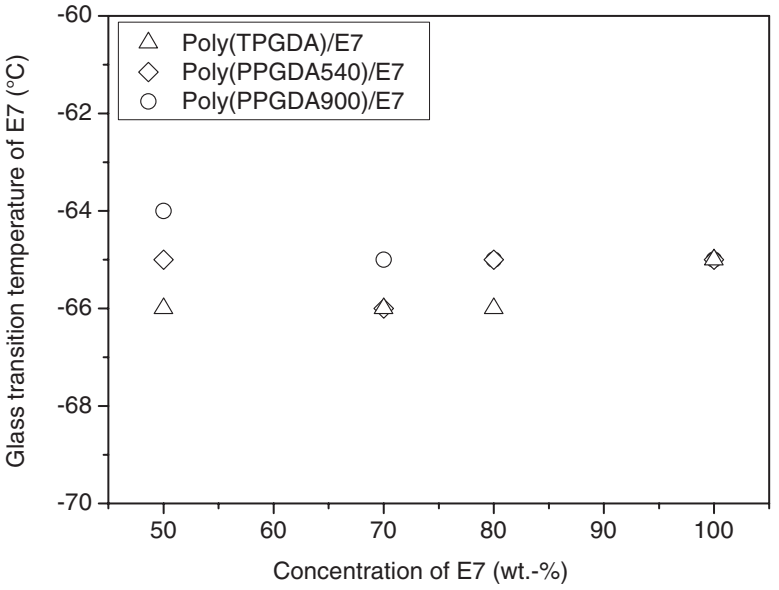

Figure 6. Variation of the LC glass transition temperature for the three monomer/LC systems as function of E7 content.

followed by poly(PPGDA540) and poly(PPGDA900), which present much lower network densities. As a consequence, the glass transition temperatures decease in the following order poly(TPGDA) ($T_g = +30°C$), poly(PPGDA540) ($T_g = -30°C$), poly(PPGDA900) ($T_g = -50°C$). In the case of the crosslinked monomer/LC systems, the poly(TPGDA)/E7 system

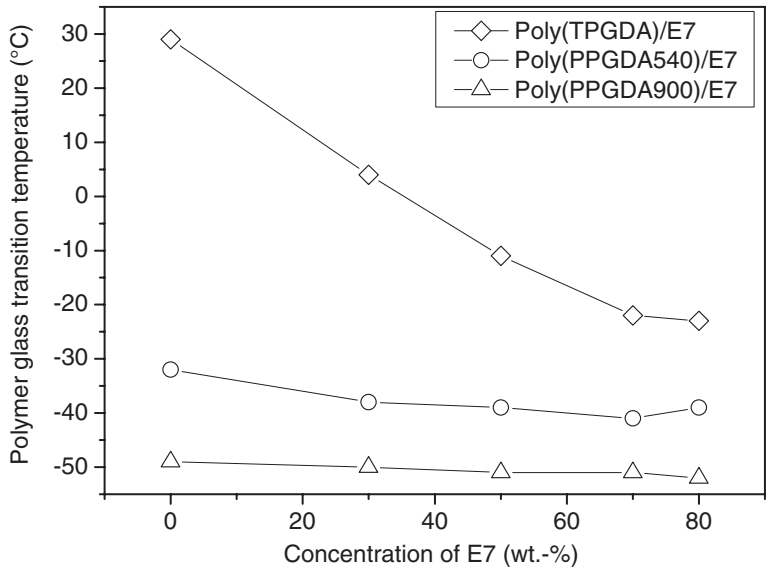

Figure 7. Dependence of the glass transition temperature of the polymer matrix on the LC concentration.

undergoes a sharp decrease of T_g with the dilution by the LC. The same remark holds for the poly (PPGDA540)/E7 system, but the decrease of the T_g is less important compared to the first system. For the poly(PPGDA900)/E7 system, the dilution effect by E7 does not affect the T_g of polymer matrix because the poly(PPGDA900) network is already loosen, and its T_g is close to that of E7. It should be kept in mind that the construction of the polymeric networks might strongly depend on the initial LC concentration. The architecture of the networks can vary as function of LC content since polymerization/crosslinking processes were carried out in situ. These results confirm that the molecular weight of the monomers directly affect the glass transition of the polymer networks formed in each system and thus the morphology of the polymer network plays an important role influencing physical properties and electro-optical responses of films made from these monomer/E7 mixtures.

4. Conclusions

The dielectric study of monomers revealed that the permittivity increases in the order PPGDA900, PPGDA540, TPGDA, which can be explained by the higher dipole moment of TPGDA caused by an enhanced volume density of carbonyl groups. For polymerized systems, increasing the LC concentration causes an increase of the conductivity. Indeed, the LC, due to its chemical structure, present higher values of conductivity than those of various acrylic polymer matrices. The contribution of the LC to dielectric phenomena becomes especially important for samples destinated for electro-optical measurements. Modeling of electrical conductivity was carried out by Arrhenius and (VTF) models and it has been shown, that both models are applicable to describe the conductivity effects in acrylic systems.

Studies by optical microscopy, carried out on monomer/LC blends, clearly indicate the strong relationship between morphology, temperature and LC content. The determination of the phase separation limit is particularly useful for the preparation of samples for electro-optical studies. Interestingly, in the case of electro-optical films with 70 wt.-% E7, the glass transition temperatures for the corresponding polymer matrix were found to be quite below room temperature, whereas the LC glass transition temperature was not affected.

References

[1] Doane, J. W., & Bahadur, B. (1990). *World Scientific.* Singapore, 361.
[2] Li, W., Cao, Y., Cao, H., Kashima, M., Kong, L., & Yang, H. (2008). *Journal of Polymer Science, Part B: Polymer Physics*, *4613*, 1369.
[3] Maschke, U., Coqueret, X., & Benmouna, M. (2002). *Macromol. Rapid Comm.*, *23*, 159.
[4] Kitzerow, H. S. (1994). *Liquid Crystals*, *16*, 1.
[5] Vaz, N. A., Smith, G. W., & Montgomery, G. P. (1987). *Liq. Cryst.*, *146*, 17.
[6] Crawford, G. P., & Zumer, S. (1996). *Dans Liquid Crystals in Cornpiex Geometries,* Taylor and Francis, London.
[7] Drzaic, P. S. (1986). *J. Appl. Phys.*, *60*, 142.
[8] Doane, J. W., Vaz, N. A., Wu, B.-G., & Zumer, S. (1986). *Appl. Phys. Lett*, *48*, 269.
[9] Vaz, N. A., & Montgomery, G. P. (1987). *J. Appl. Phys.*, *62*, 8.
[10] West, J. L. (1985). *Liquid crystalline polymers*, Ed. A. Weiss, C. K. Ober, Washington, 475.
[11] Merck, *Liquid Crystals,* Licrilite Brochure. (1994).
[12] Tarry, H. A., *The Refractive Indices of Cyanobiphenyl Liquid Crystals*, Merck Ltd, Merck.
[13] Douali, R., Legrand, C., Faye, V., & Nguyen, H. T. (1999). *Mol. Cryst. Liq. Cryst., 328*, 209.
[14] Heavin, S. D., & Fung, B. M. (1991). *SPIE*, *1455*, 13.
[15] Roussel, F., Maschke, U., Coqueret, X., & Buisine, J. M. (1998). *C. R. Acad. Sci.,* Paris, 449.

[16] Roussel, F., Maschke, U., Coqueret, X., & J. M. Buisine. (1998). *Liq. Cryst.*, *24*, 555.
[17] Russel, G. M., Paterson, B. J. A., & Imrie, C. T. (1995). *Chem. Mater.*, *7*, 2185.
[18] Nwabunma, D., Kim, K. J., Lin, Y., Chien, L. C., & T. Kyu. (1998). *Macromolecules*, *31*, 6806.
[19] Derouiche, Y., Ghefir, S. A. K., Dubois, F., Douali, R., Legrand, C., Azzaz, M., & Maschke, U. (2010). *International Review of Physics*, *4*, 163.
[20] Derouiche, Y., Dubois, F., Douali, R., Legrand, C., & Maschke, U. (2011). *Mol. Cryst. Liq. Cryst.*, *541*, 201.
[21] Bobade, R. S., Pakade, S. V., & Yawale, S. P. (2009). *J. Non-Cryst. Solids*, *357*, 2410.
[22] Joykumar Sing, T. H., & Bhat, S. V. (2003). *Bull. Mat. Sci.*, *26*, 707.
[23] Bamford, D., Reich, A., Dlubek, G., Alloin, F., Sanchez, J. Y., & Alam, M. A. (2003). *J. Chem Phys.*, *118*, 9420.
[24] Bamford, D., Reich, A., Alam, M. A., Meyer, W., Galvoska, P., & Rittig, F. (2003). *J. Chem. Phys.*, *115*, 7260.
[25] Klinkalai, W., Kawahara, S., Marwanta, E., Mizumo, T., Isono, Y., & Ohno, H. (2006). *Solid State Ionics*, *177*, 3251.
[26] Vogel, H. (1922). *Phys. Z.*, *22*, 645.
[27] Fulcher, G. S. (1925). *J. Am. Chem. Soc.*, *8*, 339.
[28] Tamman, G., Hesse, W., & Anorg, Z. (1926). *Allg. Chem., 156*, 245.
[29] Stepniak, I., & Andrzejewska, E. (2009). *Electrochimica Acta*, *54*, 5660.
[30] Rajendran, S., & Uma, T. (2000). *Bull. Mater. Sci., 23*, 27.
[31] Kim, S. H., Kim, J. Y., Kim, H. S., & Chao, H. N. (1999). *Solid State Ionics*, *116*, 63.
[32] Williams, M. L., Landell, R. F., & Ferry, J. D. (1955). *J. Am. Chem. Soc.*, *77*, 3701.
[33] Okamoto, Y., Yeh, T. F., Lee, H. S., & Skotheim, T. A. (1993). *J. Polym. Sci., Part A: Polym. Chem.*, *31*, 2573.